CHAPTER

3
Synthesis of metal doped g–C_3N_4 and characterization techniques

1. Introduction

Graphitic carbon nitride (g-C_3N_4), as a fascinating conjugated polymer, has been the hotspot in science as a metal-free and visible-light-responsive photocatalyst. Pure g-C_3N_4 suffers from insufficient sunlight absorption, low surface area and the fast recombination of photo-induced electron-hole pairs, resulting in low photocatalytic activity. Utilizing the thermal polymerization process, metal-doped g-C_3N_4 has been formed and the formed catalysts employed for the degradation of methyl orange under visible light. The produced catalysts have been examined using a variety of characterization techniques and by experimental means. The lowering of band gap and improved photocatalytic activity of the as-prepared catalyst is resulted by metal doping.

2. Materials

Anhydrous *iron sulphate* (*$FeSO_4$*), *melamine* (*$C_3H_6N_6$*), *Et(OH)*, *Congo red dye* (CR) ($C_{32}H_{22}N_2Na_2O_6S_2$) were of high–purity (analytical grade) were attained from Merck, SDFCL, and SRL Chemicals Co., India. Entire solutions were formed with high pureness double distilled water (DDW).

3. Synthesis of g–C_3N_4

Graphitic carbon nitride (g–C_3N_4) was prepared through thermal polymerization method. 5 g of melamine was used in an alumina crucible with a muffle furnace overheated at 600°C for 6 h (Figure. 3.1). Finally, we collected the yellow precipitation nanopowder to do further characterization.

4. Synthesis of metal doped g–C_3N_4

Graphitic carbon nitride (g–C_3N_4) mixed with iron sulphate was prepared through thermal polymerization method. 5 g of melamine and 250 mg chemical having metal were used in an alumina crucible with a muffle furnace overheated at 600°C for 6 h. Finally, we collected the yellow precipitation nano powder to do further characterization.

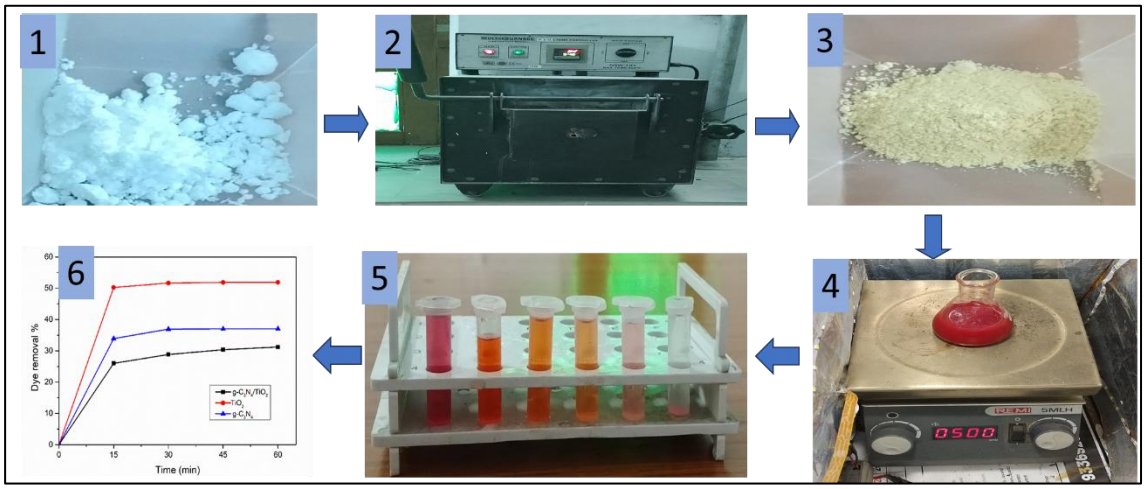

Figure 3.1 Steps of synthesis & degradation with g–C_3N_4

5. Optimization of synthesis temperature and time

Graphitic carbon nitride is synthesized at different temperatures and for different time period as previously mentioned in various literature (400°C, 500°C, 600°C and

700°C & for 4h, 5h, 6h and 7h) at same heating rate (10°C/min). Catalyst synthesized at 600°C was showing maximum removal as compared to other temperatures similarly removal was maximum for catalyst which was synthesized for 6 h. This is due to the fact that at lower temperatures less graphitic carbon nitride is formed while after 600°C graphitic carbon nitride starts to decompose in gases which lower the overall yield same thing happens with time.

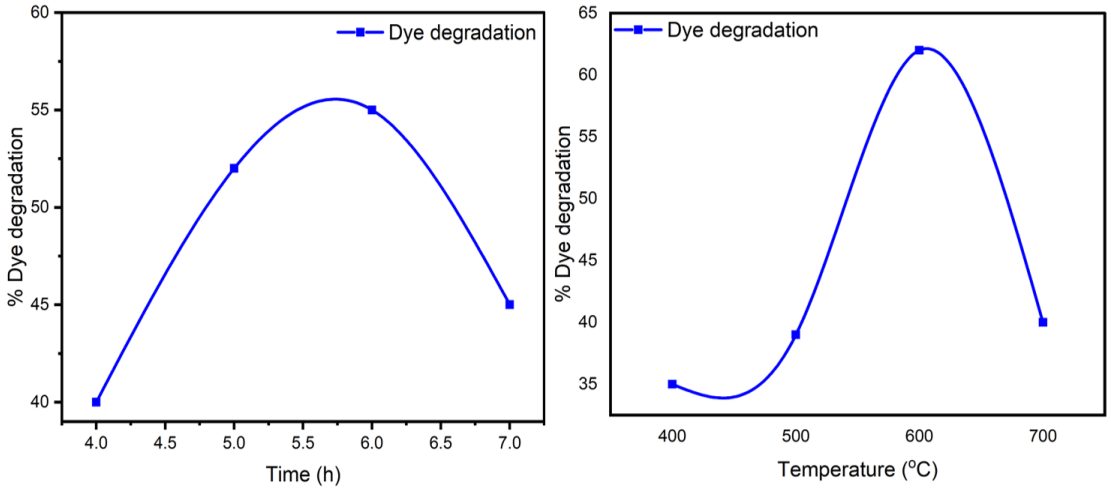

Figure 3.2 Optimization of synthesis parameters

6. Characterization techniques

6.1 X–ray Diffraction technique

X–ray was discovered by Roentgen in 1895 and was applied for structural studies in the year 1912 by Bragg. XRD is a powerful analytical technique used the determination of average grain size, lattice constants, and degree of crystallinity in a mixture of amorphous and crystalline substances. Therefore, the XRD pattern depends on the dual wave/particle nature of X–rays to obtain information about the structure of crystalline materials (Hall and Weber, 1954). This method depends on the diffraction of X–ray radiation which generally occurs only when the wavelength of the wave motion is of the

same order of magnitude as the repeat range between scattering centers. The experimental set–up of the XRD instrument is shown in Figure.3.3.

XRD is based on positive monochromatic X–rays interference and a crystalline sample. These X–rays are created by a cathode ray tube, filtered to produce monochromatic radiation, collimated to concentrate, and directed toward the sample. The interaction of the incident rays with the sample produces constructive interference when conditions of diffraction are known as Bragg's law and are represented by equation (3.1)

$$n\lambda = 2dsin\theta \tag{3.1}$$

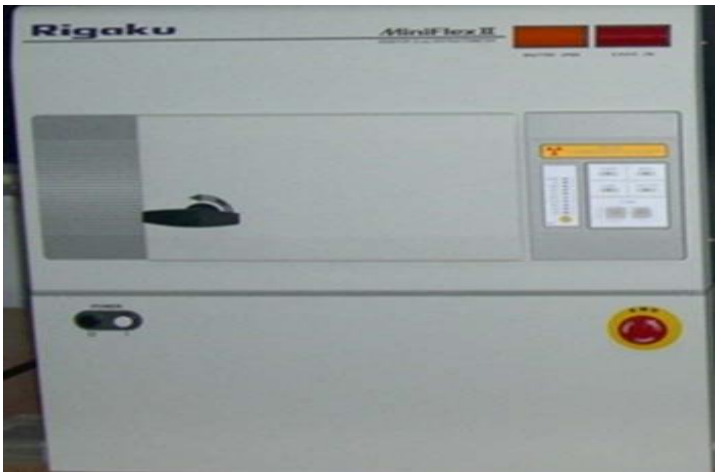

Figure 3.3 Rigaku X–ray diffractometer

Where, d – Interplanar spacing, θ – diffraction angle, λ –wavelength of X–ray and n – order of diffraction. These diffracted X–rays are then identified, measured and counted by scanning the sample through a range of 2θ angles, all possible diffraction directions of the lattice should be accomplished due to the random orientation of the powdered material. Conversion of the diffraction peaks to d spacings allows being classified of the mineral because each mineral has a set of unique d–spacings. Usually, this is attained by assessment of d–spacings with standard reference patterns i.e. JCPDS files.

XRD is most widely used for the identification of unknown crystalline materials (e.g. minerals, inorganic Compounds). Determination of unknown solid is critical to studies in geology, environmental science, material science engineering and biology.

(i) Characterization of crystalline materials.

(ii) Determination of unit cell dimensions.

(iii) Measurement of sample purity.

(iv) Determining lattice mismatch between film and substrate.

(v) Make textural measurements, such as the orientation of grains, in a polycrystalline sample.

(vi) Determine of modal amounts of minerals (quantitative analysis).

(vii) Determining the thickness, roughness and density of the film using glancing incidence x–ray reflectivity measurement and make textural measurements, such as the orientation of grains, in a polycrystalline sample.

6.1.1 Applications

We will be concentrating on the most common application of X–ray diffraction, which is the identification of crystalline substances based on their diffraction pattern. Some specific usage that we will discuss in this course are listed below:

- Single–phase material identification, including ceramics, chemical compounds, minerals, and other artificial materials.
- Multiple phases in microcrystalline mixtures identification (i.e., rocks).
- Crystal structural determination of identified materials.
- Identification and structural analysis of clay minerals.
- Recognition of amorphous materials in partially crystalline mixtures below is some more advanced techniques. Some of these will be addressed in an

introductory fashion in this course. Many are left for more advanced individual study.

- Crystallographic structural analysis and unit–cell calculations for crystalline materials.
- Quantitative determination of phases by whole–pattern refinement.
- Determination of crystallite size from analysis of peaks broadening.
- Determine of crystalline shapes from study of peak symmetry.
- Study of thermal expansion in crystal structures using in–situ heating stage equipment.

6.2 Fourier Transform Infrared Spectroscopy

6.2.1 Introduction

Fourier transform infrared spectroscopy is based on simple mathematical technique to resolve a complex wave into its frequency components. FTIR is rapidly becoming a common feature in modern spectroscopy laboratories. With the advent of inexpensive microcomputers, wide range of commercial FTIR spectrometers with very different specification is now available. In frequency domain spectroscopy, the radiant power G is recorded as a function of frequency (Nauert et al., 2018). On the other hand, the change in the radiant power f(t) is recorded as a function of time t in the case of time domain spectroscopy. The spectroscopy converts the time domain plot into a frequency domain spectrum.

The FTIR spectra of the samples were recorded using the slandered KBr pellet methods at room temperature by using Broker Tensor 27 FTIR spectrometer (Figure. 3.4). The required amount of pre–heated sample was pressed using a hydraulic press under a pressure of 2 tons cm^{-2} to make a pellet. This pellet was used to record the infrared

spectrum in the range of 400–4000 cm^{-1}. The pellet was scanned 50 times at 4 cm^{-1} resolution. The spectrum was recorded as % transmittance against wavenumber.

Figure 3.4 Broker Tensor 27 FTIR spectrometer

6.2.2. *Experimental setup*

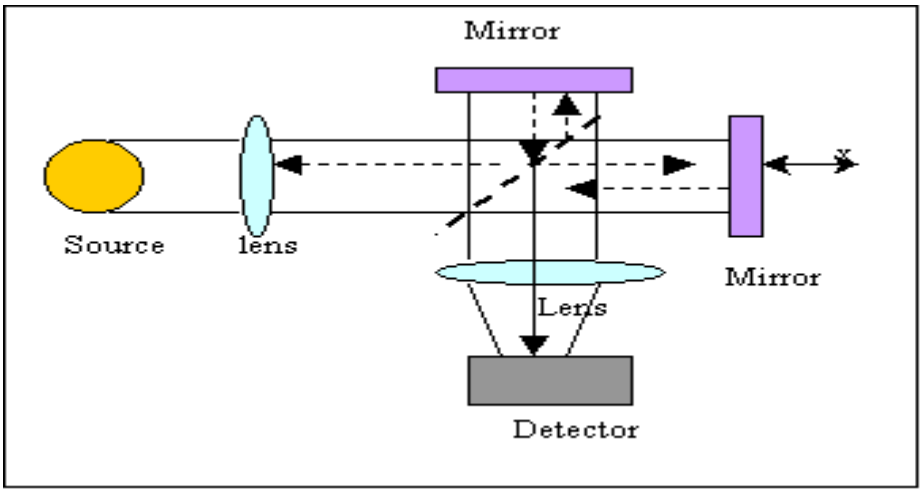

Figure 3.5 Block diagram of an FTIR spectrometer

The basic components of a Fourier transform spectrometer are given in Figure 19. The Michelson interferometer consists of a source S, a beam splitter B and two plane mirrors M_1 and M_2 is capable of to and fro movements. The beam splitter allows 50% of

the radiation to mirror M_1 and the other 50% to mirror M_2. The two beams are reflected back to B where they recombine with 50% going to the source and the other 50% going to the sample (MEE – Material Evaluation and Engineering).

The Fourier transform spectrometer is similar to Michelson interferometer but one of the two fully–reflecting mirrors is movable, allowing a variable delay (in the travel time of the light) to be included in one of the beams.

If mirror M_1 is moved towards or away from B, the sample and detector will see an alternation in intensity. If two different monochromatic frequencies υ_1 and υ_2 are used instead of one, a more complicated interference pattern would follow when M_2 is moved. A Fourier transform of the resultant signal would give the two original with the appropriate intensities. Extending this, a white light produces an extremely complicated interference pattern which can be transformed back to the original frequency distribution. If the recombined beam is directed through sample absorption will show up as gaps in the frequency distribution which on transformation gives a normal absorption spectrum. In the experiment, the detector signal is collected into a multichannel computer while mirror M_2 is moved. The computer then carries out the Fourier transform of the stored data and plots it on a paper.

6.3. Scanning Electron Microscopy

The scanning electron microscope (SEM) is a microscope that uses electrons instead of light to form an image. Since their development in the early 1950's, scanning electron microscopes have developed new areas of study in the medical and physical science communities. The scanning electron microscope has many advantages over traditional microscopes. The SEM has a large depth of field, which allows more of a specimen to be in focus at one time. The SEM also has much higher resolution, so closely

spaced specimens can be magnified at much higher levels. Because the SEM uses electromagnets rather than lenses, the researcher has much more control in the degree of magnification.

6.3.1. Principles of scanning electron microscope (SEM)

Significant amounts of kinetic energy are carried by accelerated electrons in a SEM, and as the incident electrons in the solid sample decelerate, this energy is released as a range of signals resulting from electron–sample interactions (Figure. 3.6). These signals include photons (characteristic X–rays used for elemental analysis and continuum X–rays), visible light (cathodluminescence–CL), heat, backscattered electrons (BSE), diffracted backscattered electrons (EBSD) that are used to determine crystal structures and orientations of minerals, and secondary electrons (which produce SEM images). Both backscattered and secondary electrons are frequently used in sample imaging. Backscattered electrons are best used to illustrate compositional contrasts in multiphase samples, while secondary electrons are best suited for displaying morphology and topography on samples (i.e. for rapid phase discrimination).

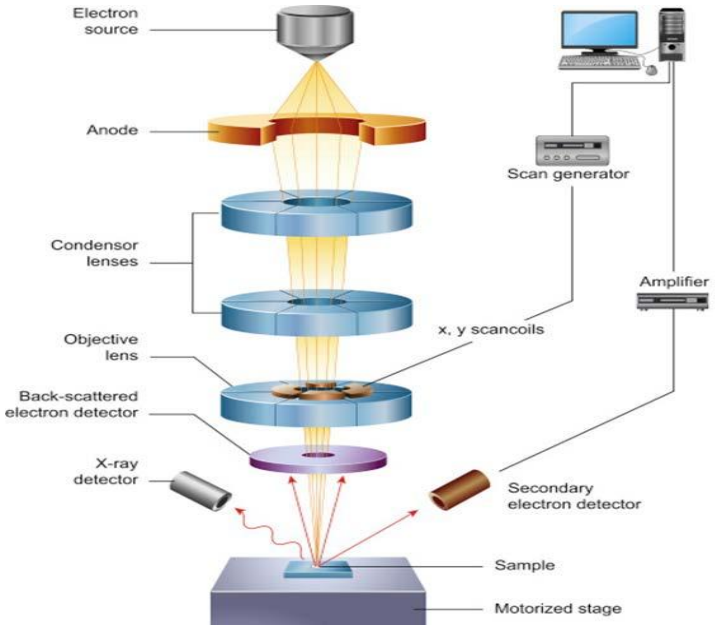

Figure 3.6 Schematic diagram of a scanning electron microscope

6.4 Energy–dispersive X–ray spectroscopy

This technique, used for the elemental analysis of the sample and also to find out the purity of the sample. The spectroscopy will show the presence of elements with the percentage of atoms and masses. The excitation of an electron from the source will interact with the sample and give results, this is the principle of EDX spectroscopy. In the EDX spectroscopy, the peak will seem with the relevant position using electromagnetic emission of the spectrum. The energy sources used in the EDX spectrum, which can give electron excitation like an X–ray beam of light irradiated to the sample. The electron presence in the atom will get excited by absorbing the energy sources which are bound to the valence shell of the electron cloud of an atom. The photon of energy excites the electron to a higher energy level and gives spectra.

6.4.1 Applications

- Bonding, Adhesion, delaminating investigations.
- Impurity detection, isolation, and identification.

- Defect analysis and Product imperfection.
- Filler, fiber, pigment, additive distribution, and orientation.
- Poisoning, and elemental distribution.

6.5 UV– vis Diffuse Reflectance Spectroscopy

UV–Vis Diffuse Reflectance spectroscopy is a very useful technique to study metals, semiconductors, and insulators in bulk, thin–film, colloid, and nanostructures forms. Generally, in the case of the semiconductor material, the absorption spectrum exhibits a sharp edge at a definite point of incident photon energy (hν) that can be ascribed to the transition of an excite electrons from valance band to conduction band, no absorption takes place. At some critical photon energy, a sudden rise in absorption is observed as the energy of the photon is enough to eject the electrons to conduction band minimum. At a still shorter wavelength or higher energy, photons continue to get absorbed (Raymond and Corkill, 1994; Tendulkar, 2006). The absorbed intensity as a function of wavelength from 200–800 nm is suitable to study electronic structure and transition between valance and conduction band. The bandgap of synthesized catalysts was calculated using Tauc's Equation.

$$\alpha h\nu = A(h\nu - E_g)^n \tag{3.2}$$

where α is the absorption coefficient, hν is the photon energy, A is constant, and n value depends on transition type. Further, the insight of the band structure of as–synthesized photocatalyst can be deduced semi–empirically using the theory of mulikene electronegativity.

$$E_{CB} = \chi - E_e - 0.5E_g \tag{3.3}$$

$$E_{CB} = E_{CB} + E_g \tag{3.4}$$

Where E_{VB} and E_{CB} are conduction and valence band edge, χ is absolute electronegativity which is the geometric mean of a constituent of semiconductor material, E_e is the energy associated with the free electron in hydrogen scale and E_g is the formidable band gap energy value of semiconductor material.

In the present study, the absorbance was performed with a UV–visible spectrophotometer to determine the photocatalytic activity of the synthesized samples. The optical properties have been studied using the UV–vis diffuse reflectance spectroscopy Perkin Elmer Lambda 25 spectrometer. The experimental setup of the UV–vis diffuse reflectance spectroscopy is shown in Figure. 3.7.

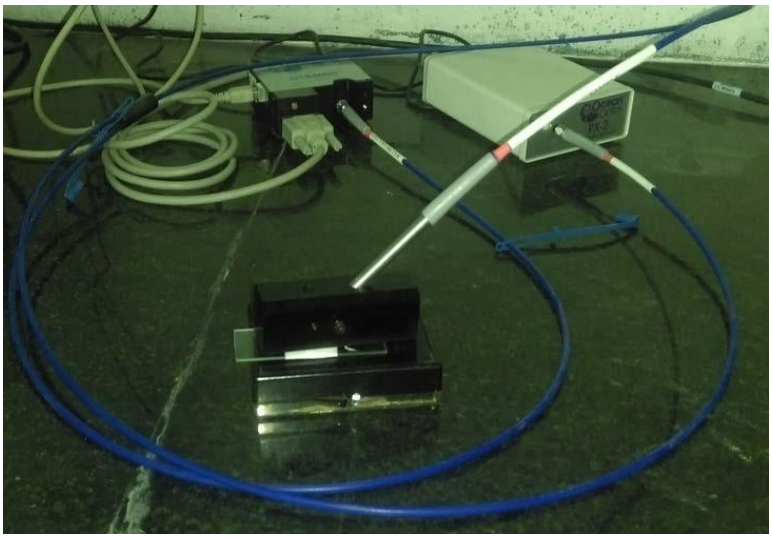

Figure 3.7 UV– Vis Diffuse Reflectance Spectrophotometer

7. Photocatalytic Reactor

The visible light photoreactor (Figure 3.8) is made up of a cubic box with reflective inner surface and from top desired light source can be clamped. Form top light source is being replaced for corresponding light experiment. At the inner side of lower face, a stirrer with hot plate is placed to maintain the temperature in the range of 25–30ºC. This reactor set–up was used in all the experiments. The source of light was a white LED light with power source 9W, 20W and 50 W. tungsten. Light penetrates a solution positioned 15 cm

from the light source, with illuminance measured at 3240 lx, 7200 lx, and 18000 lx for 9W, 20W, and 50W light sources, respectively. Photocatalysts were introduced into the dye solution, which was stirred continuously in a setup with water movement capabilities. Prior to initiating the photocatalytic reaction, the mixture underwent dark adsorption for 30 minutes to attain equilibrium of organic dye adsorption on the photocatalyst surface. Subsequently, the suspension was stirred and exposed to visible light irradiation. Samples (2 ml) were periodically withdrawn, centrifuged at 5000 rpm to separate the photocatalyst, and analyzed with a UV–vis spectrometer to measure the concentration of CR dye in the solution.

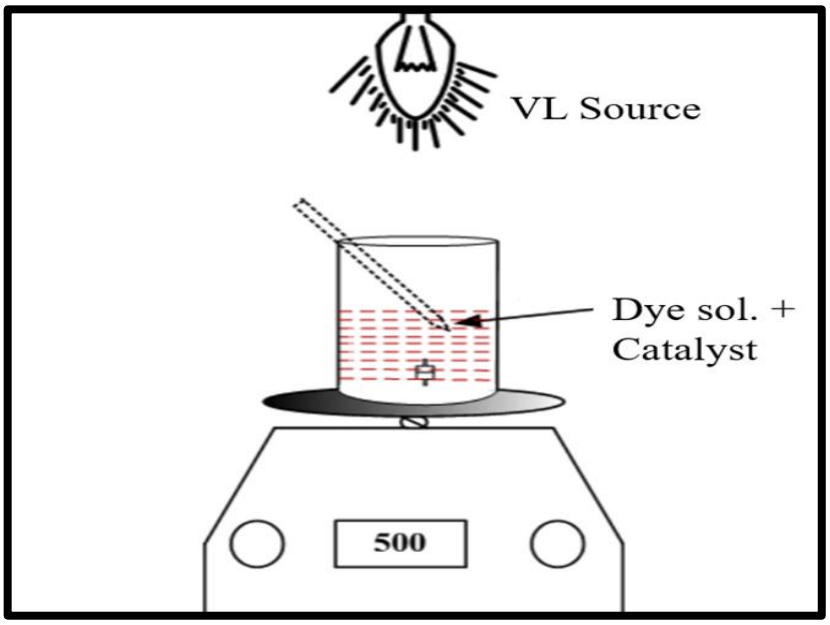

Figure 3.8 Schematic image of the reactor setup for photodegradation.